Materials Research Bulletin 44 (2009) 2014–2021

Contents lists available at ScienceDirect

Materials Research Bulletin

journal homepage: www.elsevier.com/locate/matresbu

From iron(III) precursor to magnetite and *vice versa*

M. Gotić *, T. Jurkin, S. Musić

Division of Materials Chemistry, Ruđer Bošković Institute, P.O. Box 180, HR-10002 Zagreb, Croatia

ARTICLE INFO

Article history:
Received 7 October 2008
Received in revised form 27 April 2009
Accepted 2 June 2009
Available online 9 June 2009

Keywords:
A. Oxides
B. Chemical synthesis
C. Mössbauer spectroscopy
C. Electron microscopy
D. Microstructure

ABSTRACT

The syntheses of nanosize magnetite particles by wet-chemical oxidation of Fe^{2+} have been extensively investigated. In the present investigation the nanosize magnetite particles were synthesised without using the Fe(II) precursor. This was achieved by γ-irradiation of water-in-oil microemulsion containing only the Fe(III) precursor. The corresponding phase transformations were monitored. Microemulsions (pH ~ 12.5) were γ-irradiated at a relatively high dose rate of ~22 kGy/h. Upon 1 h of γ-irradiation the XRD pattern of the precipitate showed goethite and unidentified low-intensity peaks. Upon 6 h of γ-irradiation, reductive conditions were achieved and substoichiometric magnetite ($\sim Fe_{2.71}O_4$) particles with insignificant amount of goethite particles found in the precipitate. Hydrated electrons (e_{aq}^-), organic radicals and hydrogen gas as radiolytic products were responsible for the reductive dissolution of iron oxide in the microemulsion and the reduction $Fe^{3+} \rightarrow Fe^{2+}$. Upon 18 h of γ-irradiation the precipitate exhibited dual behaviour, it was a more oxidised product than the precipitate obtained after 6 h of γ-irradiation, but it contained magnetite particles in a more reduced form ($\sim Fe_{2.93}O_4$). It was presumed that the reduction and oxidation processes existed as concurrent competitive processes in the microemulsion. After 18 h of γ-irradiation the pH of the medium shifted from the alkaline to the acidic range. The high dose rate of ~22 kGy/h was directly responsible for this shift to the acidic range. At a slightly acidic pH a further reduction of $Fe^{3+} \rightarrow Fe^{2+}$ resulted in the formation of more stoichiometric magnetite particles, whereas the oxidation conditions in the acidic medium permitted the oxidation $Fe^{2+} \rightarrow Fe^{3+}$. The Fe^{3+} was much less soluble in the acidic medium and it hydrolysed and recrystallised as goethite. The γ-irradiation of the microemulsion for 25 h at a lower dose rate of 16 kGy/h produced pure substoichiometric nanosize magnetite particles of about 25 nm in size and with the stoichiometry of $Fe_{2.83}O_4$.

1. Introduction

Iron oxides (a group name for iron hydroxides, oxyhydroxides and oxides) are widespread in nature, in soils, sediments and aquatic systems. Synthetic iron oxides have found different applications as pigments, catalysts, sensors, magnetic materials, etc. In chemical laboratories research in iron oxides is generally focused on (a) the phase transformation mechanisms which can also simulate some natural processes, and (b) the synthesis of iron oxide powders or films with derived properties for possible applications. Recently, researchers have focused their attention on the phase transformation of iron oxides under the influence of γ-radiation [1–7].

In a previous work [1] we have synthesised almost pure magnetite nanoparticles using a γ-irradiated water-in-oil microemulsion. The starting iron chemicals were $FeCl_3/FeSO_4$ and the precipitation agent was a strong organic alkali, tetramethylammonium hydroxide (TMAH). A molar ratio of Fe^{2+}:Fe^{3+} = 2:3 was used, which was higher than for the stoichiometric magnetite. Only non-magnetic iron phase (poorly crystallised goethite) was formed in the microemulsion without γ-irradiation. In an aqueous solution the Fe^{2+} ions quickly oxidised by taking up oxygen dissolved in water. Moreover, even with a properly deoxygenated solution, water molecules alone can oxidise Fe^{2+}. Vigorous stirring leads to the oxidation of Fe^{2+} to Fe^{3+} due to the dissolution of oxygen and/or a frequent contact of Fe^{2+} with oxygen in air. The pH of the solution above 3 favours the oxidation of Fe^{2+}. A slow alkali addition as well as the excess of Fe^{2+} ions in the medium also favour the formation of ferric species. Fe^{2+} in magnetite particles can easily oxidise in atmospheric conditions, especially if magnetite particles are in the nanosize range. Magnetite particles synthesised by a wet-chemical approach are always more or less substoichiometric. The syntheses of magnetite starting from pure Fe^{3+} salts include the use of reducing agents, which can be regarded as an disadvantage. On the other hand, the γ-irradiation of the precipitation system generates an extremely high reductive power *per se* [1–7], which could be utilised on a large scale.

* Corresponding author. Tel.: +385 14561123; fax: +385 14561123.
E-mail address: gotic@irb.hr (M. Gotić).

0025-5408/$ – see front matter © 2009 Elsevier Ltd. All rights reserved.
doi:10.1016/j.materresbull.2009.06.002

In this work some new results of the phase transformation of iron(III) precursor to magnetite and *vice versa* in the γ-irradiated water-in-oil microemulsion are presented. In these experiments we avoided the use of a ferrous precursor and opted for γ-radiation that generates free radicals, which in turn promote the reductive dissolution and recrystallisation of the iron(III) precursor into magnetite. However, we found that the reduction and oxidation processes in the microemulsion occurred at the same time and that the maximum reduction condition level in the microemulsion depended not only on the absorbed dose, but also on the system's pH. It was found that the system's pH was directly linked to the dose rate. The relatively high dose rate of 22 kGy/h was able to shift the alkaline pH of the microemulsion to the acidic range after 18 h of γ-irradiation. On the other hand, even after 25 h of γ-irradiation at the lower dose rate of 16 kGy/h the pH of the microemulsion persisted in the alkaline range.

2. Experimental

The two-microemulsion technique was used for the synthesis of samples [1]. The water-in-oil microemulsion **A** containing 28 ml of cyclohexane, 3 ml of Triton X-100, 1 ml of 0.1 M aqueous solution of $FeCl_3$ as an iron precursor and 1 ml of n-penthanol. The water-in-oil microemulsion **B** containing 28 ml of cyclohexane, 3 ml of Triton X-100, 1 ml of TMAH as a precipitation agent (25 wt.% tetramethylammonium hydroxide aqueous solution) and 1 ml of n-penthanol. The water-to-surfactant-ratio (w_o) in both microemulsions was 10 ($w_o = 10$). In order to precipitate iron oxide the microemulsion **B** was poured into the microemulsion **A**. The water-in-oil microemulsion **AB** thus obtained was bubbled with N_2 for 30 min and aged in a closed flask at room temperature for 18 h (reference sample M0). In the subsequent experiments the microemulsion **AB** was bubbled with N_2 for 30 min and γ-irradiated for 1, 6 and 18 h (samples M1, M6 and M18, respectively). γ-irradiation was performed using a ^{60}Co source located in the Division of Materials Chemistry at the Ruđer Bošković Institute. The dose rate of γ-radiation was ~22 kGy/h. The exact absorbed doses were: sample M1 received the dose of 21.4 kGy, sample M6 received 129.6 kGy and sample M18 received 399.6 kGy. Also, the same microemulsion **AB** was bubbled with N_2 for 30 min and γ-irradiated for 25 h at a lower dose rate of ~16 kGy/h (sample ML25, absorbed dose 399.9 kGy). The microemulsions were destabilised by adding acetone and the precipitates were isolated by centrifugation combined with successive washing in acetone and absolute ethanol. Isolated precipitates were dried under vacuum at room temperature.

X-ray diffraction (XRD) patterns were recorded at 20 °C using APD 2000 X-ray powder diffractometer (CuKα radiation, graphite monochromator, NaI-Tl detector) manufactured by *ItalStructures*, Riva Del Garda, Italy. The XRD patterns were recorded over the 15–95° 2θ range with a 2θ step of 0.03° and a counting time per step of 17–30 s.

The thermal field emission scanning electron microscope (FE-SEM), model JSM-7000F, manufactured by *Jeol Ltd.*, was connected to the EDS/INCA 350 (energy dispersive X-ray analyzer) manufactured by *Oxford Instruments Ltd*. The transmission electron microscope (TEM), model EM 10, produced by *Opton* was also used.

^{57}Fe Mössbauer spectra were recorded in the transmission mode using a standard instrumental configuration by *WissEl GmbH* (Starnberg, Germany). The ^{57}Co in the rhodium matrix was used as a Mössbauer source. The spectrometer was calibrated at 20 °C using the standard α-Fe foil spectrum. The velocity scale and all the data refer to the metallic α-Fe absorber at 20 °C. The experimentally observed Mössbauer spectra were fitted using the *MossWinn* program.

The Fourier transform infrared (FT-IR) spectra were recorded at 20 °C using a *Perkin-Elmer* spectrometer model 2000. The specimens were pressed into small discs using a spectroscopically pure KBr matrix. The spectra were recorded using a KBr beam splitter in the mid IR region (4000–400 cm^{-1}) and a Mylar beam splitter in the far IR region (700–200 cm^{-1}).

3. Results and discussion

Ageing of the water-in-oil microemulsion containing an iron(III) precursor and a strong organic alkali (TMAH) as the precipitation agent for 18 h yielded poorly crystallised ferrihydrite (reference sample M0). The starting pH ~ 12.5 of the precipitation system was measured. Krehula et al. [8,9] synthesised acicular α-FeOOH particles from $FeCl_3$ solutions at a very high pH using TMAH as the precipitation agent. These α-FeOOH particles recrystallised on account of dissolved ferrihydrite particles, initially formed. In addition to that, the transformation of ferrihydrite or "amorphous" iron(III)-hydroxide into goethite is a fast process in the presence of TMAH [8]. For that reason the reference sample was isolated after ageing of the microemulsion for 18 h, which corresponded to the highest γ-irradiation time of the same microemulsion. The FT-IR spectrum of this reference sample M0 (Fig. 5) did not contain the characteristic FT-IR bands for goethite at about 890 and 795 cm^{-1}. In other words, ferrihydrite that precipitated instantaneously in the microemulsion did not transform into goethite within 18 h of ageing at room temperature and can be used as a reference sample for all γ-irradiated samples.

Fig. 1 shows the FE SEM micrographs of non-irradiated reference sample M0 and samples M1, M6 and M18 obtained by the γ-irradiation of the microemulsion at a relatively high dose rate of ~22 kGy/h for 1, 6 and 18 h, respectively. Sample M0 (Fig. 1a) consisted of large aggregates with no visible spherical or rod-like particles. Sample M1 (Fig. 1b) is composed of aggregates of various dimensions. Two types of particles are visible, the relatively very small pseudospherical particles and the elongated, relatively long irregular plate-like particles. Some of the aggregates consisted of no visible particles. Sample M6 (Fig. 1c) consisted of aggregates of discrete spherical particles of around 30–40 nm in size. Sample M18 (Fig. 1d) again consisted of two types of particles, discrete spherical particles and a small quantity of rod-like particles visible in the upper left side of Fig. 1d.

Fig. 2 shows TEM micrographs of samples M1 and M6. A large non-transparent aggregate and irregular plate-like particles at the periphery of Fig. 2a are visible in sample M1. Sample M6 contains pseudospherical particles of 10–15 nm in size. It should be noted here that the FE SEM size measurement of the particles of the same sample M6 showed pseudospherical particles of 30–40 nm in size (measured precisely by the cursor). The different sample dispersion during the TEM and FE SEM examinations may explain this discrepancy. In FE SEM analysis the pure powder on graphite support was analyzed in the scanning mode. In such an examination several particles are in close contact and stick together, so FE SEM identifies two or several particles as one. On the other hand, before the TEM examination powder was ultrasonically dispersed in ethanol, the suspension was dropped onto the TEM grid and analyzed in the transmission mode, so that almost every single particle could be discerned.

Fig. 3 shows XRD patterns of samples M1, M6 and M18. The XRD pattern of sample M1 showed the presence of goethite, non-crystalline phase, and unidentified peaks. The high background in the XRD patterns below 70° is assigned to the presence of a non-crystalline phase. The line assignment for goethite is in good accordance with "The International Centre for Diffraction Data" (ICDD) card no. 29-0713, which undoubtedly confirms the presence of goethite in sample M1. The *hkl* indices of goethite

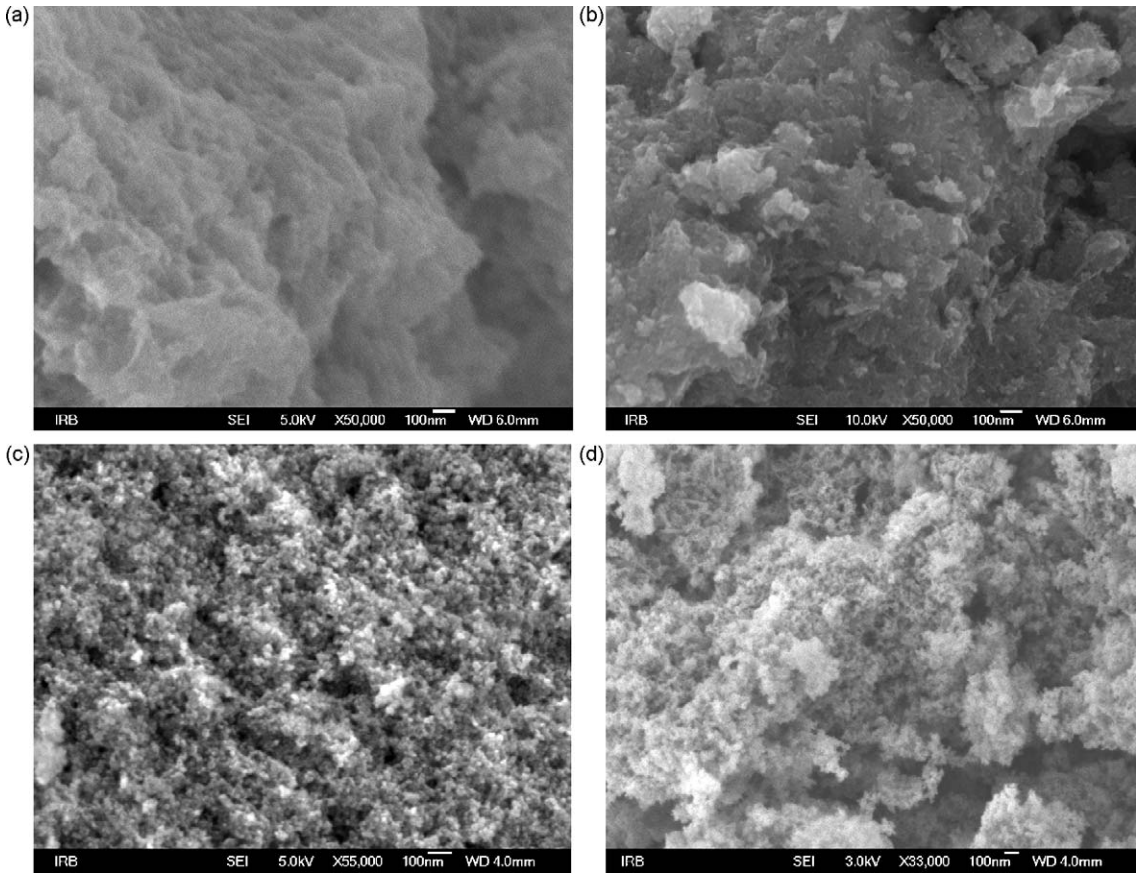

Fig. 1. FE SEM micrographs of reference sample M0 isolated after ageing of non-irradiated microemulsion for 18 h (a) and samples isolated from microemulsions γ-irradiated for 1 h (b), 6 h (c), and 18 h (d) (samples M1, M6 and M18, respectively).

are given. The Mössbauer spectrum (Fig. 4) and the FT-IR spectrum (Fig. 5) of sample with bands at 890 and 794 cm^{-1} corroborate the presence of goethite in sample M1. The relative intensities of goethite lines in sample M1 do not exactly fit the ICDD card 29-0713. This difference in relative intensities of XRD peaks may be explained by the preferential adsorption on selected plane(s) of goethite [10]. For example, tetramethylammonium cation can strongly adsorb on negatively charged goethite surfaces. The same is true of Fe^{2+} ions formed by γ-irradiation. The appearance of goethite in the form of thin irregular 2D plates (Figs. 1b and 2a) can account for the features in the corresponding XRD pattern. In the XRD pattern of sample M1, magnetite diffraction lines with Miller indices 311, 400 and 511 (denoted in sample M6) were not resolved from the goethite diffraction lines, thus magnetite was unfounded. However, sample M1 responded to the external magnetic field, thus suggesting the presence of a magnetic phase in sample M1. Since the XRD patterns did not provide any conclusive evidence of the presence of magnetite and/or ferrihydrite, the extra lines in the XRD patterns of sample M1 are assigned as unidentified (Fig. 3).

Sample M6 consists of magnetite (ICDD card 19-0629) and a very small amount of goethite (G). The *hkl* indices of magnetite are given (Fig. 2). The position of diffraction lines with Miller indices 311, 400, 422, 511 and 440 gives a lattice constant of 0.836 nm, which is typical of the substoichiometric magnetite ($\sim Fe_{2.71}O_4$) [11]. The Rietveld refinement (MAUD program) of the same XRD patterns gives similar results, a lattice constant of 0.836 nm and an average particle size of 12.8 nm. This is in very good accordance with the particle size of 10–15 nm deduced from TEM (Fig. 2b). The amount of goethite in the precipitate was estimated at 5.6 wt.%.

Sample M18 consisted of goethite and magnetite, non-crystalline phase (high background) and unidentified peaks. In sample M18 magnetite diffraction lines with Miller indices 311, 400 and 511 (denoted in sample M6) are resolved from goethite diffraction lines. The line positions yield a lattice constant of 0.839 nm, indicating stoichiometry $\sim Fe_{2.93}O_4$. The line widths are narrower than for sample M6, suggesting larger magnetite grains (about 30 nm). The diffraction lines at 37.4, 38.4, 45.8, 48.7, 65.1 and 67.1 2θ degrees are assigned to unidentified peaks.

Fig. 4 shows the Mössbauer spectra of samples M1, M6 and M18. The Mössbauer spectrum of sample M1 is characterised by one collapsing sextet and one doublet (Table 1). The collapsing sextet is fitted taking into account the distribution of hyperfine magnetic fields having an isomer shift, $\delta = 0.43$ mm s^{-1} (relative to α-Fe), a quadrupole shift, $2\varepsilon = -0.19$ mm s^{-1} and the hyperfine magnetic field, $B_{hf} = 27.4$ T. The quadrupole shift of -0.19 mm s^{-1} is typical of the magnetically ordered goethite [12,13]. The reduced hyperfine field compared with the well-crystallised goethite can be generally assigned to small particles and/or varying crystallinity of goethite. The doublet occupied 70% of the total relative area in the Mössbauer spectrum having an isomer shift, $\delta = 0.34$ mm s^{-1} and a quadrupole splitting, $\Delta = 0.70$ mm s^{-1}. Generally, the doublet can arise from any paramagnetic and/or superparamagnetic iron oxide phase, including the superparamagnetic particle of goethite and/or magnetite [13]. The bag-like shape of the Mössbauer spectrum of sample M6 (130 kGy), similar to those observed for spin glasses, is consistent with expectations for strongly agglomerated 10 nm subparticles of magnetite. The relatively high asymmetry indicates the substoichiometric magnetite ($\sim Fe_{3-x}O_4$) in accordance with the XRD patterns. The presence of goethite in the Mössbauer spectrum of sample M6 cannot be determined because the parameters of the collapsing inner sextet of substoichiometric magnetite and the sextet of goethite highly overlapped. The

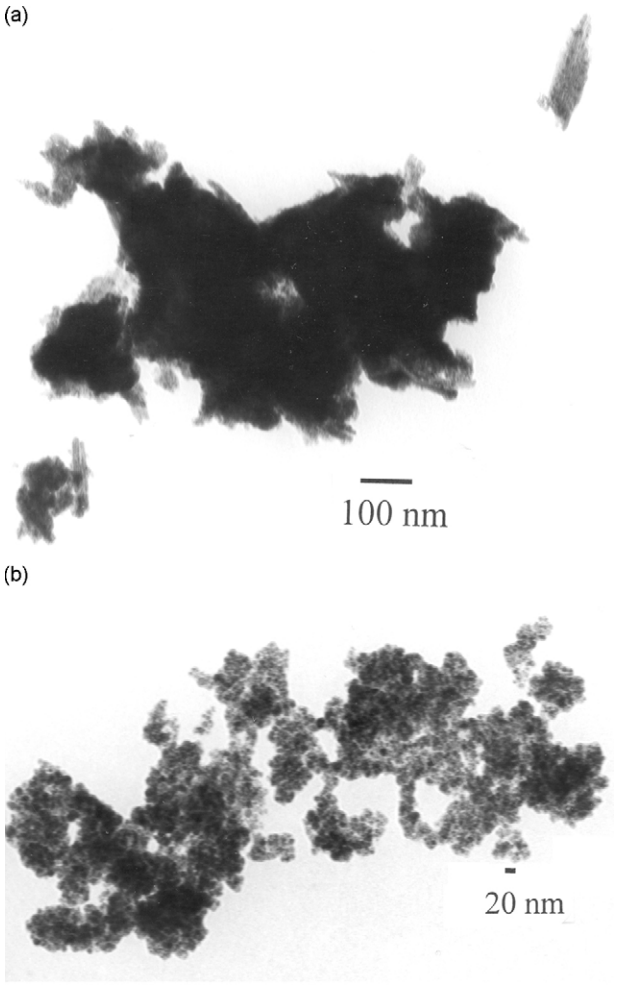

Fig. 2. TEM micrographs of sample M1 (a) and sample M6 (b).

Mössbauer spectrum of sample M18 is more complex due to the presence of the phase mixture, mixed oxidation state, size distributions and magnetic ordering. The superposition of three sextets can be recognised, a sextet of goethite and two sextets of magnetite, which is in accordance with XRD results. The presence of the doublet suggests a heterogeneous system, which is also in accordance with XRD results. The enhanced magnetic character of the spectrum compared with sample M6 indicates larger particles.

Fig. 5 shows the FT-IR spectra of reference sample M0 and γ-irradiated samples M1, M6 and M18. The bands at about 3400 and 1630 cm^{-1} correspond to H–O–H stretching and H–O–H bending vibrations of H_2O molecules incorporated into the precipitate, respectively. The shoulders at 3247 cm^{-1} in sample M0 and 3229 cm^{-1} in sample M1 correspond to O–H stretching vibrations. The broad bands at about 1550 and 1345 cm^{-1} in samples M0 and M1 are due to coordinated or adsorbed carbonate. Ferrihydrite and poorly crystallised goethite are very susceptible to CO_2 from air. Also, these bands could be related to various organic groups coordinated (chemisorbed) on the iron oxide precipitate. The sharp bands at 1490 and 949 cm^{-1} are due to physically sorbed organic groups on the surface of the precipitate. The very sharp band at 1385 cm^{-1} in sample M6 is an artifact and does not represent the FT-IR bands of the sample. The peaks at 2922 and 2 853 cm^{-1} are assigned to the asymmetric and symmetric CH_2 stretching vibration, respectively. The broad and strong bands at 599 and 436 cm^{-1} in sample M0 are related to iron oxide phase. These bands are typical of low crystalline ferrihydrite or "amorphous" iron(III)-hydroxide [14]. The FT-IR spectrum of sample M1 contains

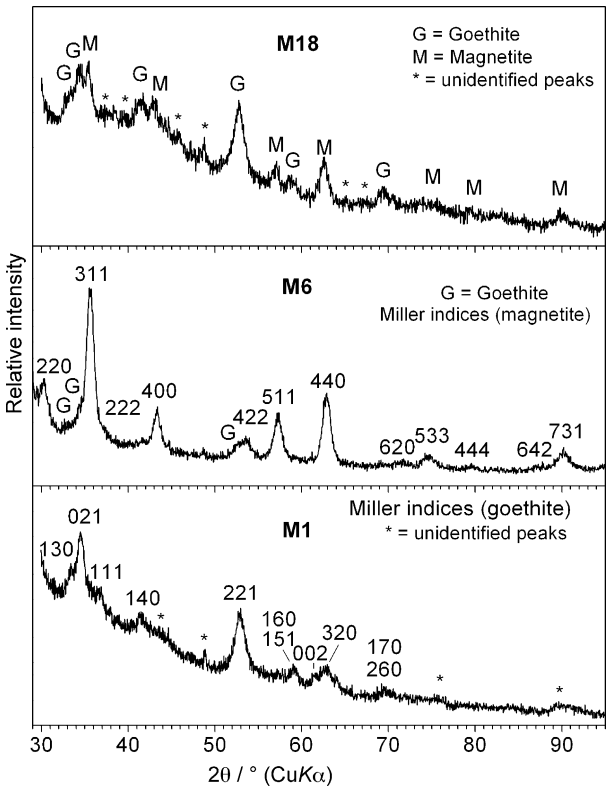

Fig. 3. XRD patterns of samples M1, M6 and M18 recorded at 20 °C.

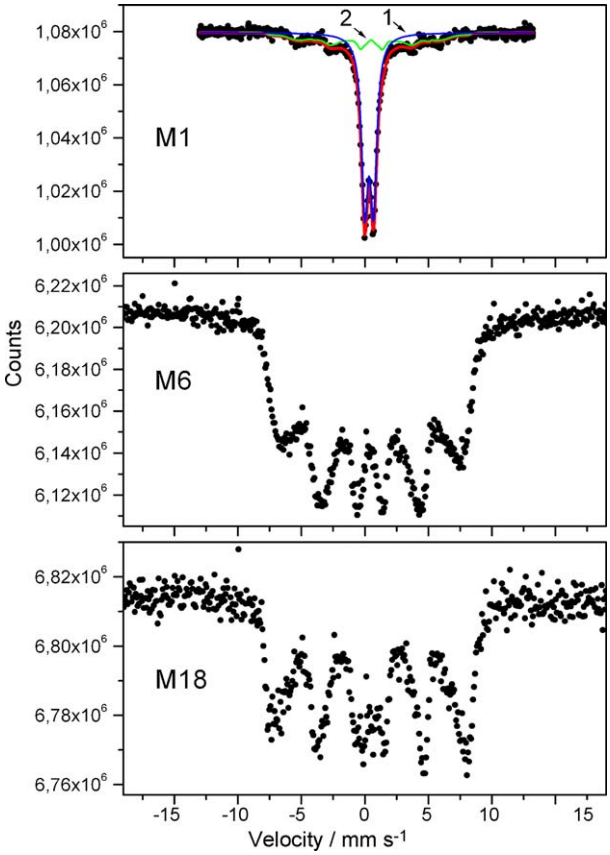

Fig. 4. Mössbauer spectra of samples M1, M6 and M18 recorded at 20 °C.

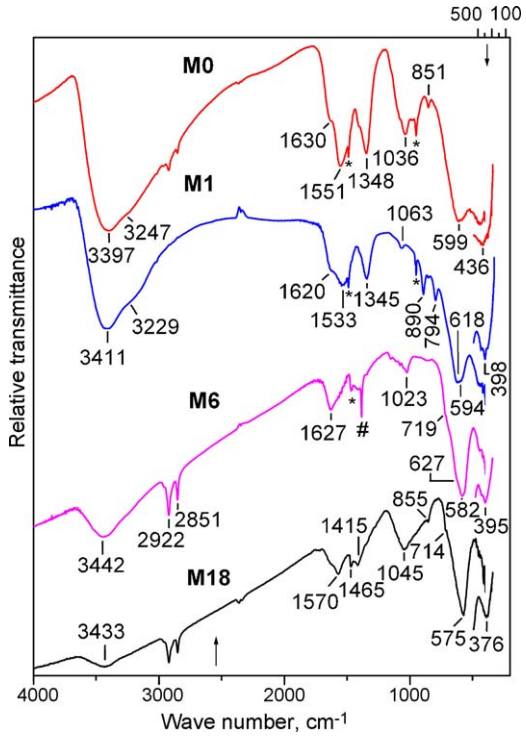

Fig. 5. FT-IR spectra of reference sample M0 and γ-irradiated samples M1, M6 and M18. The spectra were recorded using a KBr beam splitter in the mid IR region (lower scale) and a Mylar beam splitter in the far IR region (upper scale).

the characteristic bands of both goethite and magnetite. The bands at 890 and 794 cm^{-1} correspond to (Fe)–O–H in-plane bend and (Fe)–O–H out-of-plane bend in goethite [10]. The wave number difference between these two O–H bands below 100 cm^{-1} indicates poorly crystallised goethite. The most intense band at 618 cm^{-1} belongs to Fe–O stretch in FeOOH. This band is not fully separate from the magnetite band at 594 cm^{-1}. In the far IR region of sample M1 there are three bands. The most intense band in the middle is at 398 cm^{-1}, the band to the left is at 455 and the one to the right at 363 cm^{-1}. The bands at 455 and 363 cm^{-1} are not marked in Fig. 5. These three bands can be assigned to the Fe–O stretching vibration in the crystal lattice of goethite (455 and 363 cm^{-1}) and magnetite (398 cm^{-1}). Sample M6 possesses two characteristic bands of magnetite at 582 and 395 cm^{-1} [11]. The XRD patterns show that this sample contains a small fraction of goethite. However, the FT-IR spectrum of sample M6 does not contain the characteristic bands of goethite at around 890 and 790 cm^{-1}. The shoulder at 627 cm^{-1} indicates a small fraction of goethite. In sample M18 the two characteristic bands of magnetite shift to lower wave numbers (575 and 376 cm^{-1}). Like in sample M6, the characteristic bands of goethite are not clearly visible in sample M18; however, the very broad band at 1045 cm^{-1} with shoulders at 855 and 714 cm^{-1} may indicate a poorly crystallised iron oxyhydroxide phase.

Fig. 6 gives a graphic representation of the possible mechanism of an iron(III) precursor to magnetite transformation and *vice versa*. Experimental results showed a complexity of reactions involved in the precipitation of iron oxide phases in microemulsions exposed to γ-radiation. Fortunately, the iron oxide's chemistry as well as the radiation chemistry of microemulsions has been the subject of detailed studies in reference literature, so that the mechanism of phase transformations in a γ-irradiated microemulsion can be described as follows: mixing of two water-in-oil microemulsions, **A** containing cyclohexane, Triton X-100, penthanol and an aqueous solution of $FeCl_3$, and **B** of the same chemical composition except that it contained TMAH instead of $FeCl_3$, yielded poorly crystallised ferrihydrite (FH) marked as "$Fe(OH)_3$" (ferric oxide precursor). The starting pH ~ 12.5 of the precipitation system was measured.

γ-Irradiation of the microemulsion increased the energy in the system (1) and impacted both the medium (2) and the precipitate (II). The radiolysis of the organic phase generated excess electrons that crossed the oil/water interface and appeared in the aqueous phase as hydrated electrons (3) [7,15–17]. The mass of cyclohexane was 43.7 g (81.4% of the microemulsion's mass), so that much of γ-ray energy was deposited in cyclohexane. The radiolysis of the aqueous phase generated various species [18], but in the present experimental conditions the most important are hydroxyl radicals ($^{\bullet}OH$). Hydroxyl radicals were scavenged by the organic phase (3′), for example by penthanol, Triton X-100 [19] and cyclohexane. What is very important, thus formed organic radicals ($OR^{\bullet}$) highly accelerated the reductive dissolution of FH (4′) [13,18]. γ-Irradiation had a direct effect on FH nanoparticles as well (II). γ-Rays deposited energy on well-dispersed FH nanoparticles and this energy was transferred to the medium (III). As a consequence, FH nanoparticles enhanced the decomposition of the organic phase and increased the yield of hydrogen gas generation (IV) [20–22]. Generation of other reductive gases cannot be excluded. The hydrated electrons, hydrogen gas and organic radicals reduced Fe(III) to Fe(II). Once the Fe(II) was formed, it acted as a catalyst (5) [23,24] and additionally accelerated the dissolution and recrystallisation of FH into goethite [13,25]. Goethite in the presence of Fe(II) is also transformed into magnetite by the dissolution/recrystallisation mechanism [13,26,27]. Upon 1 h of γ-irradiation a mixture of goethite (G) and non-crystalline phase (NC) was formed, and unidentified peaks were also found in the XRD pattern.

The reductive processes continued (6) and after 6 h of γ-irradiation the precipitate contained almost pure 10–15 nm substoichiometric magnetite particles ($Fe_{2.71}O_4$). Due to the high dose rate (22 kGy/h) the pH of the microemulsion decreased (7) and shifted from the alkaline to the acidic range. At this high dose rate the degradation of organic phase, the formation of acidic organic intermediates [28] and a vigorous hydrolysis and reduction of Fe(III) may be responsible for such a dramatic drop

Table 1
^{57}Fe Mössbauer parameters at 20 °C calculated for sample M1 to ML25.

Sample	Fitting curve	δ (mm s^{-1})	Δ or 2ε (mm s^{-1})	B_{hf} (T)	Γ (mm s^{-1})	Relative area (%)	Phase composition
M1	1	0.34	0.70		0.61	70.0	PD or SP
	2[d]	0.43	−0.19	27.4	0.23	30.0	Goethite
ML25	1	0.29	0.00	47.6	0.41	16.3	Substoichiometric magnetite
	2	0.53	−0.09	44.5	0.47	11.6	
	3	0.48	−0.06	38.1	1.16	72.1	"Smear" subsextet

Key: δ = isomer shift given relative to α-Fe at RT; Δ or 2ε = quadrupole splitting or quadrupole shift; B_{hf} = hyperfine magnetic field; Γ = line width. *Error*: δ = ±0.01 mm s^{-1}; Δ or E_Q = ±0.01 mm s^{-1}; B_{hf} = ±0.2 T. *Remarks*: sample M1: PD = paramagnetic doublet; SP = superparamagnetic doublet; 2[d] = goethite subsextet fitted to the distribution of hyperfine magnetic fields. Sample ML25: 1 = outer subsextet of magnetite; 2 = inner subsextet of magnetite; 3 = introduced imaginary subsextet ("smear" subsextet) fitted to the distribution of hyperfine magnetic fields.

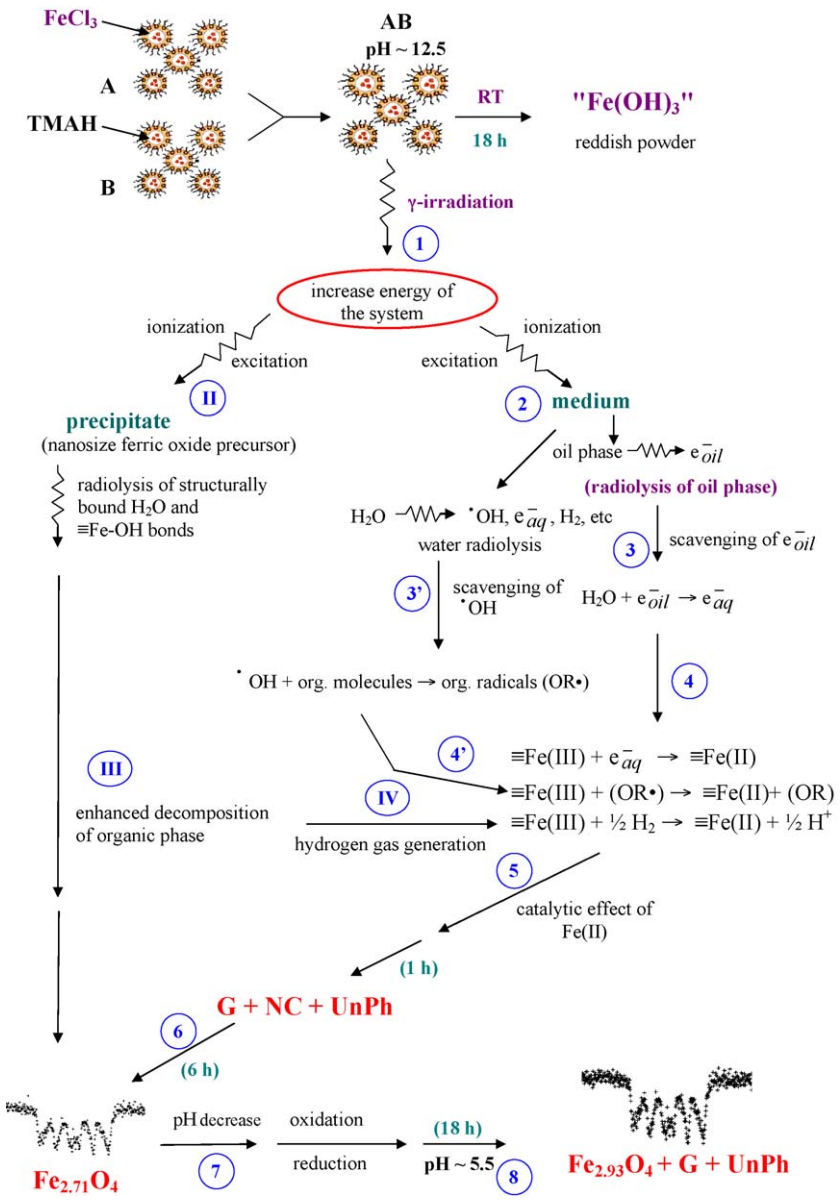

Fig. 6. Graphic presentation of a possible mechanism of iron oxide phase transformations in the γ-irradiated water-in-oil microemulsion. A description of this graphic presentation is given in Section 3. M stands for magnetite, G for goethite, UnPh for an unidentified phase and NC for a non-crystalline fraction.

in pH. Regardless of the origin of the pH decrease, this strongly influenced the oxidation–reduction conditions in the microemulsion. At a slightly acidic pH the reduction and oxidation processes occurred in the microemulsion at the same time. Further reduction of $Fe^{3+} \rightarrow Fe^{2+}$ resulted in the recrystallisation of more stoichiometric magnetite particles ($\sim Fe_{2.93}O_4$), whereas the oxidation process resulted in the recrystallisation of goethite in the precipitate. Also, in a slightly acidic medium the concentration of Fe^{2+} in the medium increased and oxidation conditions permitted the oxidation $Fe^{2+} \rightarrow Fe^{3+}$. Being much less soluble in the acidic medium, Fe^{3+} hydrolysed and recrystallised as goethite. Thus after 18 h of γ-irradiation the precipitate exhibited dual behaviour, it was a more oxidised product than the precipitate obtained after 6 h of γ-irradiation, but it contained magnetite in a more reduced form, i.e., the precipitates contained magnetite ($\sim Fe_{2.93}O_4$), goethite (G) and an unidentified phase (UnPh).

About the above mechanism one may argue that it is not clear what is the reason for a continuous pH decrease upon γ-irradiation from the initial value of 12.5 to the slightly acidic value of 5.5. It is suspected that γ-irradiation by itself is not responsible for the pH drop and that prolonged γ-irradiation affects the system only indirectly through medium acidification. In order to determine the influence of γ-irradiation on the microemulsion's pH, we γ-irradiated the microemulsion for 25 h at a lower dose rate of 16 kGy/h (sample ML25). The microemulsion's pH after 25 h of γ-irradiation was about 9, i.e., stayed in the alkaline range. Fig. 7 shows microstructural characterisation of sample ML25. The FE SEM image (Fig. 7a) shows pseudospherical particles of about 30–50 nm in size, as measured precisely with the cursor (*Jeol* software). The TEM image (Fig. 7b) shows two large soft aggregates consisting of nanosize particles. The three discrete particles of irregular shape in a close contact just above the size mark are well visible. The size of these particles is estimated at ca. 25 nm. However, if we look at these three particles in close contact as one big particle, the particle size will be about 40 nm. In other words, for reasons discussed above the FE SEM identifies these three particles as a single particle and gives the average particle sizes of

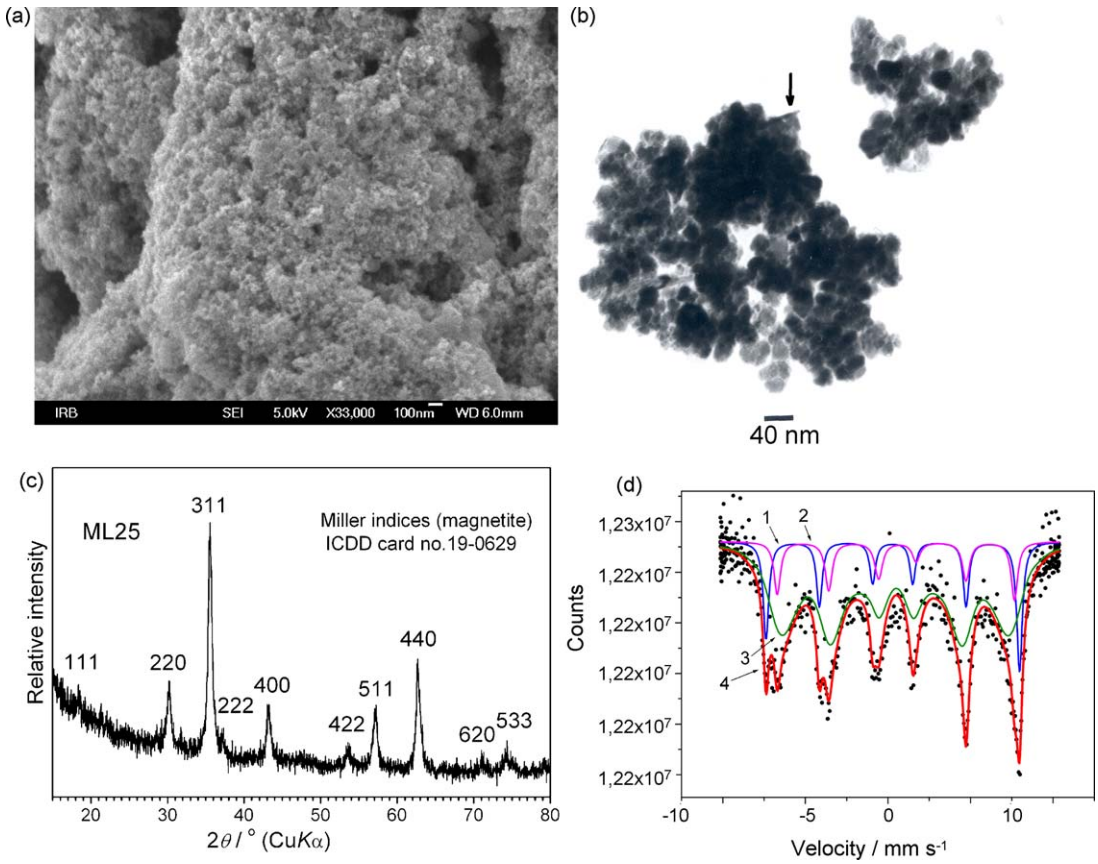

Fig. 7. Microstructural characterisations of sample ML25 obtained by γ-irradiation of water-in-oil microemulsion for 25 h at a dose rate of 16 kGy/h. FE SEM image (a), TEM micrograph (b), XRD patterns (c) and Mössbauer spectrum (d). The dots in Mössbauer spectrum are experimental data, subsextet 1 is the outer sextet of magnetite, subsextet 2 is the inner sextet of magnetite, subsextet 3 is the imaginary subsextet (''smear'' subsextet) introduced to improve the fit. The curve 4 is the summation of all three subspectra.

30–50 nm. It should be noted that sample ML25 was not absolutely pure from the morphological point of view. Amidst the huge quantity of pseudospherical particles the one rod-like particle at the top of the larger aggregate can be discerned (indicate by arrow). Fig. 7c shows the XRD patterns of sample ML25. The XRD patterns of this sample are in accordance with the ICDD card no. 19-0629 (magnetite). The declared lattice constant of magnetite is $a = 8.396$ Å. The calculated lattice constant of sample ML25 is $a = 8.37$ Å and can be characterised as substoichiometric magnetite with the approximate stoichiometry of $Fe_{2.86}O_4$. By applying the Scherrer formula to the width of the 311, 400, 511 and 440 lines at half maximum, the crystalline size of 21 nm can be estimated. Fig. 7d shows the Mössbauer spectrum of sample ML25. This spectrum is fitted to three sextets (Table 1). The number 1 corresponds to the outer subsextet of magnetite, the number 2 corresponds to the inner subsextet of magnetite, and the number 3 corresponds to the imaginary subsextet introduced to improve the fit (''smear'' subspectrum). Since the XRD patterns proved the existence of pure magnetite, a possible physical implication of thus introduced imaginary sextet is to compensate for the collapsing nature of the spectrum and the broad distribution of magnetic fields at the octahedral positions (subsextet 2). The relative intensities of sextets 1 and 2 imply the substoichiometric nature of magnetite particles [29].

Thus the microemulsion's pH γ-irradiated for 25 h stayed in the alkaline range, whereas the pH of microemulsion γ-irradiated for 18 h shifted from the alkaline to the acidic range. Both microemulsions received the same absorbed dose of 400 kGy. It is therefore clear that the relatively high dose rate of 22 kGy/h was able to shift the microemulsion's pH to the acidic range, unlike the prolonged duration of γ-irradiation (25 h) at a dose rate of 16 kGy/h. γ-Irradiation, i.e., the dose rate was directly responsible for the shift of the microemulsion's pH from the alkaline to the acidic range. Furthermore, samples ML25 and M18 that had received the same dose were not alike, but samples ML25 and M6 were very much alike, because both samples precipitated in alkaline conditions. Sample ML25 was structurally characterised as pure substoichiometric magnetite ($Fe_{2.86}O_4$), whereas sample M6 was characterised as substoichiometric magnetite ($Fe_{2.71}O_4$) with a very small amount of goethite impurity. Sample M18 that had precipitated at a high dose rate in the acidic medium had the best magnetite stoichiometry ($Fe_{2.93}O_4$); however, that sample contained a lot of goethite as impurity. Generally, these results imply that by controlling the absorbed dose as well as the dose rate of γ-irradiation one can control the phase composition, stoichiometry and particle size of the precipitate.

4. Conclusions

The water-in-oil microemulsions containing only the iron(III) precursor were γ-irradiated at a relatively high dose rate of 22 kGy/h. In the γ-irradiated water-in-oil microemulsion the reduction and oxidation processes occurred in the microemulsion at the same time.

Two main effects of γ-irradiation on the precipitate were observed: *(i)* the amount of magnetite in the precipitate increased up to 6 h of γ-irradiation and then the process reversed decreasing the amount of magnetite in the precipitate, and *(ii)* the

stoichiometry of magnetite continuously improved with γ-irradiation, being about ~$Fe_{2.71}O_4$ after 6 h of γ-irradiation and $Fe_{2.93}O_4$ after 18 h of γ-irradiation. Therefore, after 18 h of γ-irradiation the precipitate exhibited dual behaviour, it was a more oxidised product than the precipitate obtained after 6 h of γ-irradiation, but it contained magnetite in a more reduced form.

It is presumed that not just hydrated electrons (e^-_{aq}), but also organic radicals and hydrogen gas as radiolytic products were responsible for the reductive dissolution of iron oxide in the microemulsion and the reduction $Fe^{3+} \rightarrow Fe^{2+}$.

γ-irradiation, i.e., the high dose rate of 22 kGy/h was directly responsible for the shift of the medium's pH from the alkaline to the acidic range. The γ-irradiation of the microemulsion for 25 h at the lower dose rate of 16 kGy/h yielded pure substoichiometric nanosize magnetite particles of ca. 25 nm in size and with $Fe_{2.83}O_4$ stoichiometry.

The present investigation has demonstrated the possibility of applying γ-irradiation in the synthesis of nanosize magnetite particles starting only from Fe^{3+} ions. By controlling the absorbed dose and dose rate of γ-irradiation one can control the phase composition, stoichiometry and size of magnetite particles.

Acknowledgments

The authors wish to express their gratitude to Dr. Elisabeth Tronc for her critical reading of this manuscript and her valuable suggestions and comments. The authors also wish to thank Dr. Tatjana Prebeg for making Transmission Electron Microscopy (TEM) measurements and Mr. M. Blažević for the technical assistance on γ-irradiation.

References

[1] M. Gotić, T. Jurkin, S. Musić, Colloid Polym. Sci. 285 (2007) 793–800.
[2] S. Wang, H. Xin, Radiat. Phys. Chem. 56 (1999) 567–572.
[3] Y. Ni, X. Ge, Z. Zhang, Q. Ye, Chem. Mater. 14 (2002) 1048–1052.
[4] S. Seino, T. Kinoshita, Y. Otome, T. Maki, T. Nakagawa, K. Okitsu, Y. Mizukoshi, T. Nakayama, T. Sekino, K. Niihara, T.A. Yamamoto, Scripta Mater. 51 (2004) 467–472.
[5] S. Seino, T. Kinoshita, Y. Otome, T. Nakagawa, K. Okitsu, Y. Mizukoshi, T. Nakayama, T. Sekino, K. Niihara, T.A. Yamamoto, J. Magn. Magn. Mater. 293 (2005) 144–150.
[6] E.B. Gracien, Z. Ruimin, X. LiHui, L.K. Kanza, I. Lopaka, J. Radioanal. Nucl. Chem. 270 (2006) 473–478.
[7] Q. Chen, X. Shen, H. Gao, J. Colloid Interface Sci. 312 (2007) 272–278.
[8] S. Krehula, S. Popović, S. Musić, Mater. Lett. 54 (2002) 108–113.
[9] S. Krehula, S. Musić, J. Cryst. Growth 310 (2008) 513–520.
[10] G.N. Subbanna, C. Sudakar, T.R.N. Kutty, Mater. Chem. Phys. 78 (2003) 43–50.
[11] M. Gotić, G. Koščec, S. Musić, J. Mol. Struct. 924–926 (2009) 347–354.
[12] E. Tronc, Private communication.
[13] R.M. Cornell, U. Schwertmann, The Iron Oxides Structure, Properties, Reactions Occurrences and Uses, Wiley-VCH Verlag GmbH & Co. KgaA, Weinheim, 2003.
[14] S. Musić, M. Gotić, S. Popović, J. Mater. Sci. 28 (1993) 5744–5752.
[15] S. Adhikari, R. Joshi, C. Gopinathan, J. Colloid Interface Sci. 191 (1997) 268–271.
[16] G. Wu, Y. Katsumura, N. Chitose, Z. Zuo, Radiat. Phys. Chem. 60 (2001) 643–650.
[17] R. Joshi, T. Mukherjee, Radiat. Phys. Chem. 66 (2003) 397–402.
[18] G.V. Buxton, T. Rhodes, R.M. Sellers, Nature 295 (1982) 583–585.
[19] J. Perkowski, J. Mayer, J. Radioanal. Nucl. Chem. 157 (1992) 27–36.
[20] S. Seino, T.A. Yamamoto, R. Fujimoto, K. Hashimoto, M. Katsura, S. Okuda, K. Okitsu, J. Nucl. Sci. Technol. 38 (2001) 633–636.
[21] D. Meisel, in: Proceedings of a Technical Meeting Held in Notre Dame, Indiana, USA, 13–17, September 2003, (2004), pp. 5–14.
[22] N.H. Sagert, P.J. Dyne, Can. J. Chem. 45 (1967) 615–627.
[23] A.G.B. Williams, M.M. Scherer, Environ. Sci. Technol. 38 (2004) 4782–4790.
[24] H.D. Pedersen, D. Postma, R. Jakobsen, O. Larsen, Geochim. Cosmochim. Acta 69 (2005) 3967–3977.
[25] N. Yee, S. Shaw, L.G. Benning, T.H. Nguyen, Am. Mineral. 91 (2006) 92–96.
[26] E. Tronc, P. Belleville, J.-P. Jolivet, J. Livage, Langmuir 8 (1992) 313–319.
[27] J.-P. Jolivet, P. Belleville, E. Tronc, J. Livage, Clays Clay Miner. 40 (1992) 531–539.
[28] S.-J. Zhang, H.-Q. Yu, L.-X. Wu, Chemosphere 57 (2004) 1181–1187.
[29] M. Gotić, S. Musić, Eur. J. Inorg. Chem. (2008) 966–973.